



HDM, interfacing thermal analysis and ambient ionisation mass spectrometry

Gage P. Ashton¹ · Lindsay P. Harding¹ · Gareth M. B. Parkes¹

Received: 16 December 2021 / Accepted: 11 March 2022 / Published online: 6 April 2022
© The Author(s) 2022

Abstract

Thermomicroscopy (aka hot-stage microscopy) has been shown to be an excellent complimentary tool when used in conjunction with other analytical techniques, such as DSC and TGA. The optical data obtained from thermomicroscopy aid in the elucidation of complex events, often seen in many thermoanalytical profiles. Here, a system linking hot-stage microscopy and direct analysis in real-time mass spectrometry is described. This combination allows the simultaneous detection of both physical and chemical properties of a material as it is heated. Results showcasing the benefits of this combination include the thermal separation of energetic materials, the analysis of 3D printer filaments, and the profiling of trace materials including paint chips and fibres.

Keywords Thermomicroscopy · Ambient ionisation mass spectrometry · Instrumentation · Hot-stage microscopy · Trace materials

Abbreviations

AIMS	Ambient ionisation mass spectrometry
DART-MS	Direct analysis in real-time mass spectrometry
DESI	Desorption electrospray ionisation
DSC	Differential scanning calorimetry
EIC	Extracted ion chromatograms
FDM	Fused deposition modelling
FTIR	Fourier transform infrared spectroscopy
GIST	Gas-ion separator tube
HDM	Hot-stage microscopy direct analysis in real-time mass spectrometry
PET	Polyethylene terephthalate
PETN	2,2-Bis[(nitrooxy)methyl]propane-1,3-diy dinitrate
PLA	Polylactic acid
Py-GC-MS	Pyrolysis gas chromatography mass spectrometry
RDX	1,3,5-Trinitroperhydro-1,3,5-triazine
RGB	Red, green, blue colour values
STA	Simultaneous thermal analysis

TGA	Thermogravimetric analysis
TG-MS	Thermogravimetric analysis, coupled with mass spectrometry
TNT	2-Methyl-1,3,5-trinitrobenzene

Introduction

The field of thermal analysis is well explored, with many thermoanalytical techniques standing the test of time for their ease of sample preparation, broad scope of applications, and general user-friendly nature [1].

The underpinning concepts of thermal analysis are relatively simple, namely the exploration of a given property as a function of temperature [2]. Of course, this has led to a wealth of instrumentation types available to the analyst today, mass changes can be explored using TGA [3], enthalpic events can be followed via DSC [4], and more unconventional events such as sound generation may even be followed using thermosonimetry [5].

With so many techniques available, there is reduced scope for development of thermal analysis instrumentation that hasn't been explored previously. A clear direction forwards is through the hybridisation, often termed hyphenation, with other scientific equipment. Still, this concept is not novel and has been successfully explored for decades

✉ Gage P. Ashton
G.P.Ashton@hud.ac.uk

¹ Thermal Methods Research Unit (TMRU), Department of Chemical Sciences, University of Huddersfield, Huddersfield HD1 3DH, UK

now, giving rise to extremely powerful methods such as STA and TG-MS [6, 7].

Thermomicroscopy, aka hot-stage microscopy is a technique widely used in the pharmaceutical sector, making use of both transmitted light and polarising light microscopy [8, 9]. Thermomicroscopy can provide complementary data to other thermoanalytical techniques, allowing the visualisation of events as the sample is heated, potentially aiding with the deconvolution of complex processes [10]. More recently, developments have been made by the incorporation of thermomicroscopy with other techniques such as FTIR [11], DSC [12], and mass spectrometry [13].

Separately, a recent movement within the mass spectrometry community is focused with so called ambient ionisation mass spectrometry (AIMS) [14]. Interest in these ambient methods started to gain attention around 2004–2006, with the introduction of techniques such as desorption electrospray ionisation (DESI) and direct analysis in real time (DART) [15, 16]. Again, the underpinning idea is a simple one, obtaining mass spectrometry data from a sample, with little to no sample preparation, whilst at atmospheric pressure. In short, samples are positioned in front of an ionisation source, the resultant analyte ions are generated via technique-specific mechanisms, and these ions are pulled into the mass spectrometer for detection [17]. These ionisation methods are typically much softer than traditional electron ionisation, often generating intact molecular ions, or their adducts, aiding overall with the speed and ease of interpretation of resultant mass spectra [18].

The study described here interfaces thermal analysis with ambient ionisation mass spectrometry, a technique combination that allows the exploration of a sample's physical and chemical information simultaneously. The technique utilises a combination of hot-stage microscopy and direct analysis in real-time mass spectrometry (termed HDM herein). A range of examples have been selected to show the benefits of this combination.

Materials and methods

Instrumentation

HDM

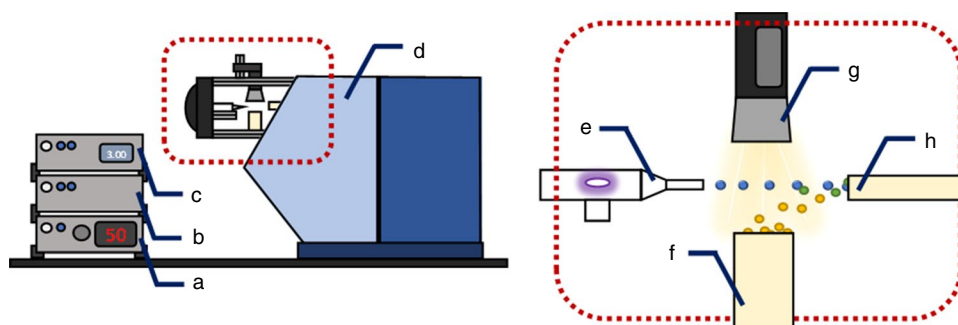
The equipment has been described elsewhere [19], however, an overview of the instrumentation is provided here and is further supported by Fig. 1. The HDM interface has four key parts, the ionisation source (Fig. 1e), the hot-stage (Fig. 1f), a digital microscope (Fig. 1g), and the atmospheric pressure mass spectrometer inlet (Fig. 1h).

A custom ambient ionisation source has been developed based on direct analysis in real time (DART). Here, a flow of gas (typically nitrogen or helium, 0–1 L min⁻¹) may be passed through the ionisation source where it interacts with high voltage electrodes, forming a corona-to-glow like discharge. This interaction generates a metastable flux that is directed across the surface of the hot-stage.

Samples are typically placed within aluminium, Inconel, or ceramic crucibles (*ca.* 5 mm ID) and are placed into the hot-stage. The temperature of the hot-stage is controlled via a PID routine, using a type K thermocouple as the input. The output consists of a series of nichrome resistive heating wires, controlled via a solid-state relay (SSR), driven by a pulse width modulated (PWM) signal from an Arduino microcontroller. As samples are heated, analytes become thermally desorbed and interact with the metastable flux passing directly above the hot-stage. The generated analyte ions are then drawn into the atmospheric pressure inlet of the mass spectrometer for detection.

Throughout the experiment micrographs (photographs of the sample) may be taken at fixed time or temperature intervals, allowing visualisation of any physical processes occurring as the sample follows the temperature programme. Additionally, real-time colour data (in the form of red, green, blue (RGB)) are extracted and recorded as a function of time or temperature, aiding with revealing subtle morphological sample changes.

Fig. 1 A schematic of the instrumentation used in this study. **a** hot-stage power regulator, **b** microcontroller, **c** high voltage and gas controller, **d** mass spectrometer, **e** ionisation source, **f** hot-stage, **g** microscope, and **h** atmospheric pressure mass spectrometer inlet



The system is controlled by software written in-house (Visual Studio 2019, Microsoft) by the development team. Here, both power and temperature control experiments may be selected, allowing controlled heating and cooling of the hot-stage.

The HDM interface has been coupled to an ion trap mass spectrometer (Bruker, esquire HCT), with a gas-ion separator tube (GIST) interface and a low volume pump to assist in pulling analyte ions towards the mass spectrometer inlet. The mass spectrometer was set to scan over 15–1500 m/z , and ions of interest were extracted for the extracted ion chromatograms (EICs) shown throughout. The ion trap was set into alternating polarity mode to allow for the detection of both positive and negative ions throughout each experiment.

Figure 2 shows example temperature profiles from the hot-stage. Controlled heating can be achieved at heating rates between 0.1 and 200 °C min^{-1} from 30 to 750 °C (Fig. 2a). Heating, cooling and isothermal periods can be set throughout the temperature programme, allowing precise control over the sample temperature (Fig. 2b).

Materials

Calibration standards

Temperature calibration standards used to calibrate the hot-stage were obtained from LGC, indium (LGC2601), tin (LGC2609) and lead (LGC2608). Additionally, a sample of high purity aluminium (99.999%, Goodfellow) was used as the upper temperature calibration standard.

Energetics materials

Solutions of 2-Methyl-1,3,5-trinitrobenzene (TNT), 2,2-Bis[(nitrooxy)methyl]propane-1,3-diyl dinitrate (PETN), and 1,3,5-Trinitroperhydro-1,3,5-triazine (RDX) (CRM in acetonitrile, Cerilliant) were deposited to leave 100 ng of each material on a smooth tiled surface following evaporation. Once the residual solvent had evaporated, a fibrous brass tool was used to collect residues from the surface via mechanical abrasion. These fibres were then cut from the abrasive tool and added directly into an aluminium thermal analysis crucible. The sample was then heated between 30 and 250 °C at a heating rate of 50 °C min^{-1} .

FDM filament

Sections of polylactic acid 3D printer filament (PLA, Zortrax) were cut and added into alumina crucibles for HDM analysis, showing the exposed cut surface towards the microscope. The filament was then heated at a rate of 10 °C min^{-1} between 30 and 500 °C. Additional confirmatory measurements were performed using both a TGA (Mettler-Toledo,

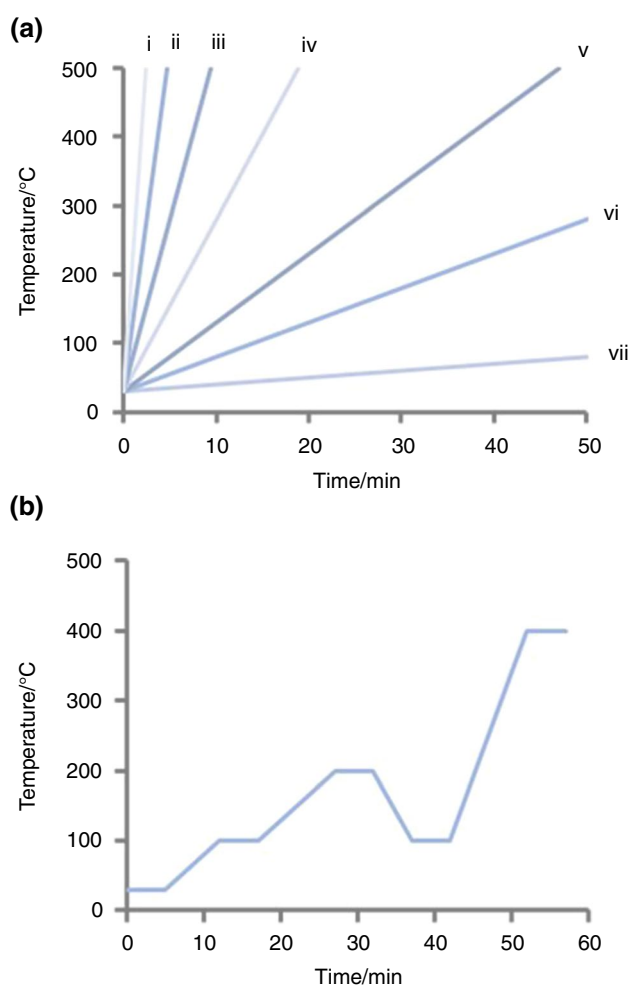


Fig. 2 Temperature profiles obtained from the HDM interface. **a** heating rate (β) comparisons (i) 200, (ii) 100, (iii) 50, (iv) 25, (v) 10, (vi) 5, and (vii) 1 °C min^{-1} . **b** An example of a multi-step temperature programme

TGA/SDTA851e) and a DSC (Mettler-Toledo, DSC821) following the same temperature programme. Sample masses of approximately 5 mg were used each time.

Paint chips

To explore the applicability of HDM to the analysis of paint chips, two similarly shaded red spray paints were obtained from a local store (“bright red”, Wilkinson) and (“cherry red”, Rust-oleum). To prepare the paint chips, several thin coats of each spray paint were applied to individual microscope slides and allowed to air dry for 24 h. A scalpel was then used to scratch the surface of the microscope slide, and the paint chips were collected and stored in individual sample vials.

Samples of the paint chips were individually added to aluminium crucibles, until masses of approximately 1 mg

were reached. The samples were then analysed using HDM between 30 and 600 °C, at a heating rate of 50 °C min⁻¹.

Polyester fibres

A section of a polyester fibre (1 mg) was cut from a bulk textile standard (Testfabrics Inc., USA) and added directly into the aluminium analysis crucible. The sample was then heated at 50 °C min⁻¹ between 30 and 450 °C.

Calibration

Temperature calibration of the hot-stage is achieved by monitoring s-l phase changes within samples of high purity metals, a standard method for the temperature calibration of many thermoanalytical instruments [20].

Here, samples ranging in masses between 5 and 50 mg are heated at fixed rates, typically to 50 °C above the expected melting transition. As the sample undergoes the s-l transition, the metallic surface relaxes, giving rise to a step change in the red, green, blue colour data (RGB) associated with a surface reflectance change. This is further confirmed by reviewing the micrographs for notable morphological changes. An example calibration profile is shown in Fig. 3. Here, the melting transition of aluminium is noted by a step change in the colour profile, and the surface smoothing noted in the micrographs.

Based on the melting transition values of several metals, a regression equation is generated and applied to the hot-stage for calibration of the sample temperature.

The mass spectrometer was calibrated in accordance with manufacturer's guidelines. Both mass and detector calibrations were performed over the range of 100–2700 *m/z* using TuneMix (Agilent, Cheadle, UK) solution (diluted 1: 10 v/v in acetonitrile).

Results and discussion

Energetic materials

Ambient ionisation methods have been extremely successful in the detection of a range of energetic materials directly from a variety of objects and surfaces [21, 22]. However, since many explosives and pyrotechnics exist as a mixture, without any separation methods such as chromatography, the resultant mass spectra could be potentially difficult to interpret.

Figure 4 shows the results from an experiment in which thermal separation of mixed energetic materials was achieved, using controlled temperature ramping at 50 °C min⁻¹ between 30 and 250 °C. All analyte ions were observed in negative ion mode. Due to differences

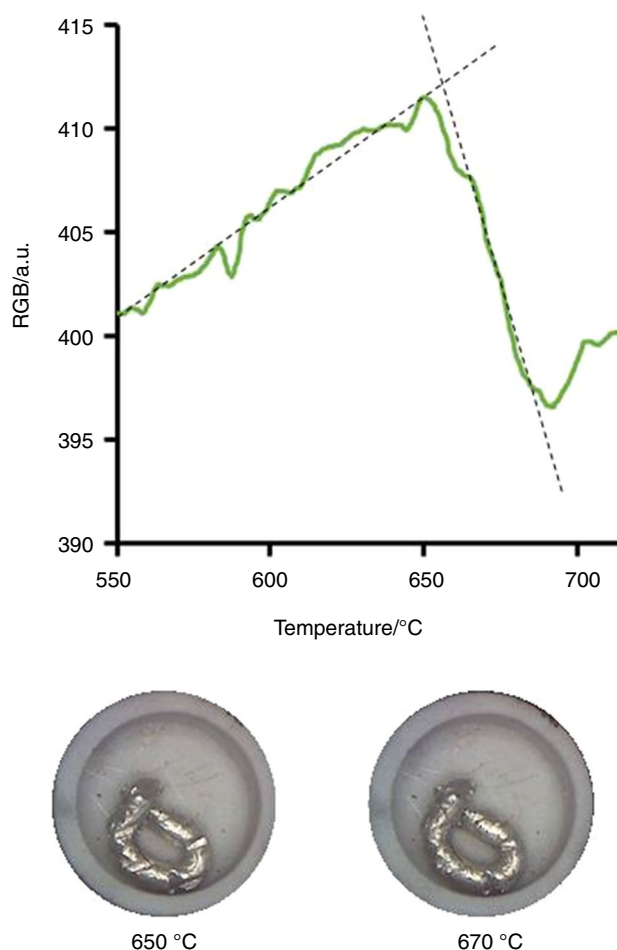


Fig. 3 The results from the calibration of the hot-stage using a sample of aluminium, the change in colour profile (RGB) has been plotted as a function of temperature. Selected micrographs show before and after the melting transition. (Sample mass, 25 mg; heating rate, 10 °C min⁻¹)

in the scale of the absolute ion intensity of each species, the profiles have been normalised for clarity. As the sample masses were at trace levels, the optical information obtained was not very revealing and has thus been omitted.

From the onset of heating, the deprotonated molecular ion of TNT [M-H]⁻ 226 *m/z* was seen to increase until reaching its maximum intensity around 105 °C before falling away. Shortly afterwards the nitrated molecular ion of PETN [M+NO₃]⁻ 378 *m/z* was then observed, reaching its peak maximum around 130 °C. Finally, the nitrated molecular ion of RDX [M+NO₂]⁻ 268 *m/z* was then seen to reach its peak maximum intensity around 160 °C. By using controlled temperature programmes like these, it is possible to separate mixed samples. Similar methods have been noted by Forbes et al., using rapid thermal separation methods in conjunction with DART-MS [23, 24]. Separation in this way could be useful for isobaric analyte ions,

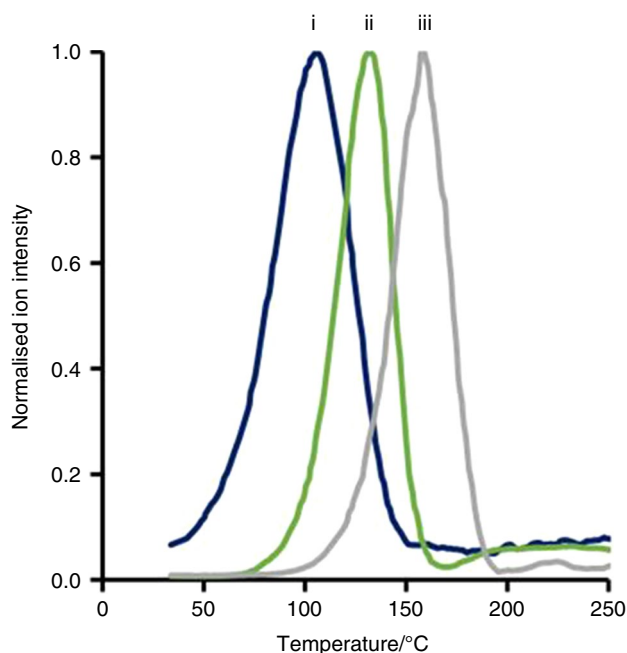


Fig. 4 HDM applied to the thermal separation of energetic materials. (i) TNT 226 m/z , (ii) PETN 378 m/z , and (iii) RDX 268 m/z . (Sample masses, 100 ng; heating rate, 50 °C min^{-1})

where it would be difficult to separate species based on their m/z ratios alone but they may be separated by their physical properties.

FDM filament

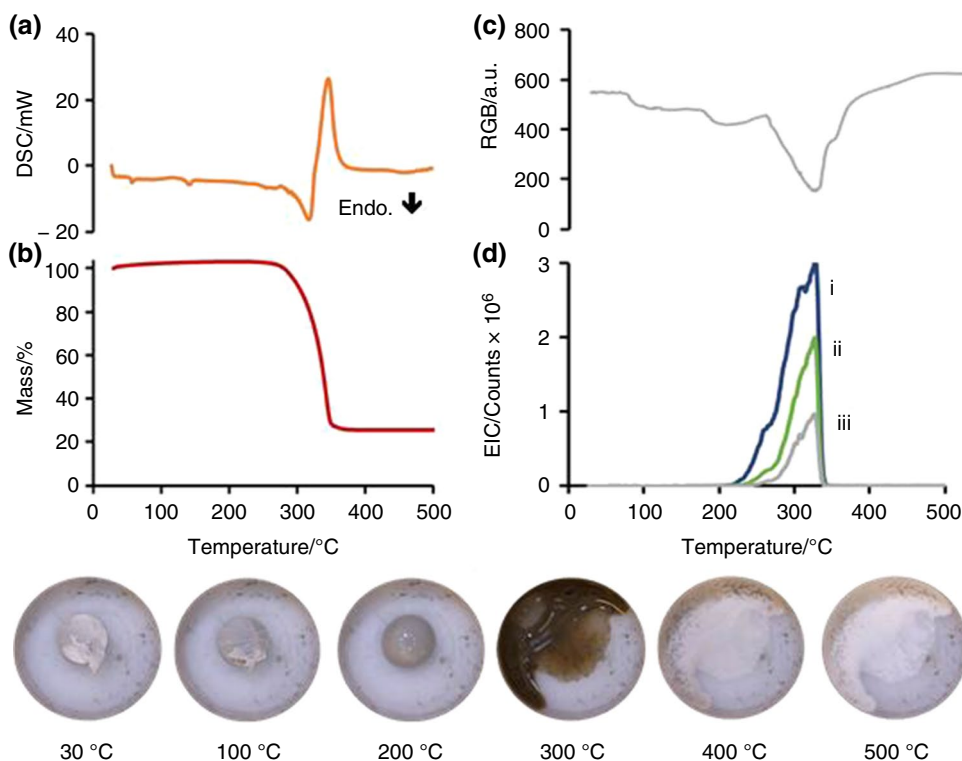
Fused deposition modelling (FDM), a branch of additive manufacturing, uses hot molten polymers forced through a printer nozzle to generate 3D printed objects [25]. Many polymer types are available for FDM-based 3D printing, such as polylactic acid (PLA), acrylonitrile butadiene styrene (ABS) and polyethylene terephthalate (PET).

Recently, many authors have been exploring how printing temperature can affect the resultant 3D printed object, paying particular focus to the extent of degradation and subsequent mechanical properties [26]. Other authors have made use of TGA and DSC as a characterisation tool to explore novel composite 3D printing materials [27].

Figure 5 draws comparisons between conventional thermal analysis methods such as DSC (Fig. 5a) and TGA (Fig. 5b), with the results obtained from HDM (Fig. 5c, d). In each case, small samples of polylactic acid (PLA) filament (*ca.* 5 mg) were analysed between 30 and 500 °C, at a heating rate of 10 °C min^{-1} .

Figure 5c focuses on the colour profile as the sample is heated. At 67 °C, a step change can be seen in the colour profile, this has been attributed to the glass transition of the polymer, as supported by the DSC (Fig. 5a), and the apparent optical relaxation, seen between micrographs 30 °C and 100 °C. The next distinctive step shown occurs around 175 °C as the sample begins to melt, supported by the micrograph at 200 °C showing a rounded bead with a

Fig. 5 Thermal analysis of polylactic acid 3D printer filament. DSC (a), and TGA (b) profiles both plotted as a function of temperature. HDM colour change (c), and extracted ion intensity profiles (d), both plotted as a function of temperature. Extracted ion profiles shown relate to ammoniated polylactic acid oligomers (i) 594 m/z , (ii) 666 m/z , and (iii) 738 m/z . Select micrographs and their transition temperatures are also shown. (Sample masses, 5 mg; heating rate, 10 °C min^{-1})



glossy surface appearance. Further heating causes a gradual darkening of the sample as the total RGB colour score is further reduced, due to the degradation of the polymer as seen between the 200 °C and 300 °C micrographs. Finally, after 310 °C, the colour begins to lighten once more as the remaining sample is exhausted, leaving behind an off-white residue attributed to the polymer's inorganic filler.

Shortly after melting, a range of ions were noted that were regularly spaced apart by 72 m/z , these have been attributed to ammoniated cyclic oligomers of PLA. Figure 5d shows the extracted ion profiles for di) 594 m/z $[C_{24}H_{32}O_{16} + NH_4]^+$, dii) 666 m/z $[C_{27}H_{36}O_{18} + NH_4]^+$, and diii) 738 m/z $[C_{30}H_{38}O_{20} + NH_4]^+$. These oligomeric species are noted to have been thermally desorbed earlier than the major mass loss shown in in the TGA profile (Fig. 5b), increasing as the polymer degrades. At the point where the colour begins to lighten again, the ion intensities fall away to background levels as the polymer becomes fully exhausted. No ions of interest were noted beyond this point, attributed to the remaining mass being a stable inorganic filler material, typically non-ionisable by soft ionisation methods such as DART.

Paint chip analysis

Paint chips can prove to be complex material to analyse, with pyrolysis gas chromatography–mass spectrometry

(Py-GC–MS) being the choice method for analysis [28]. Recently, Bridge et al. used DART-MS in the study of automotive paint analysis, drawing on statistical methods such as multivariate analysis to aid in the interpretation of complex mass spectra [29].

Figure 6 shows the analysis of two similarly coloured red spray paints using HDM. Here, dried paint chips were removed from a glass slide and added directly into the analysis pan, before being heated between 30 and 600 °C at a rate of 50 °C min^{-1} .

Initially, the starting colour of both paint chips was a similar shade of red, however, upon heating clear distinctions can be made from the colour profiles (Fig. 6ai, aii) and their corresponding selected micrographs. Both spray paints clearly melt upon heating, appearing glossy and rounded by 200 °C.

Further heating of both paint chips leads to their degradation, however, their pathways are notably different as explored by the colour profiles and micrographs. Figure 6ai, shows a major step change in the colour profile of the “cherry red” paint chip shortly after 450 °C. A sharp step in colour is observed as the paint chip degrades revealing the exposed base of the crucible, leaving minimal residue by 600 °C. The profile for Fig. 6aii (“bright red” paint chip) is a little more subtle in comparison. The onset of degradation occurs around 400 °C as the colour of the paint changes from red to a dark orange. Continued heating exhausts remaining

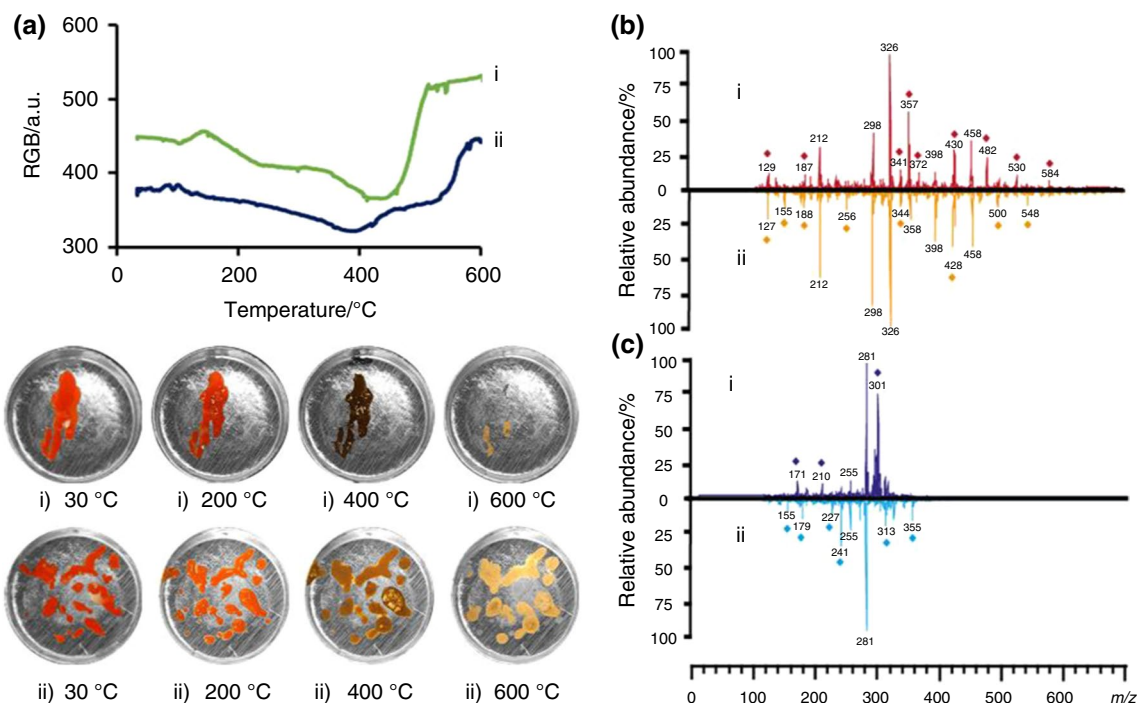


Fig. 6 The analysis of two similarly coloured paint chips studied by HDM. **a** colour change plotted as a function of temperature, **b** positive mode average mass spectra, shown as an inversion plot, and **c**

negative mode average mass spectra, shown as an inversion plot. (i) “cherry red” spray paint, (ii) “bright red” spray paint. (Sample masses, ≈ 1 mg; heating rate, 50 °C min^{-1})

material from 520 °C until a pale-yellow residue remains by 600 °C.

The ion trap mass spectrometer used in this study has ion switching capabilities, allowing both positive and negative mode mass spectra to be obtained pseudo-simultaneously. Shown in Fig. 6 are inversion plots for the averaged mass spectra in both positive (Fig. 6bi, bii) and negative (Fig. 6ci, cii) ion modes, collected over the whole analysis temperature range of 30–600 °C, with unique ions being marked by a diamond symbol.

Here, the use of colour monitoring provides additional information aiding in the discrimination of two similarly sourced samples, a feature particularly useful in scenarios where the averaged mass spectra share many ions due to a chemically similar composition.

Fibre analysis

Fibres are ubiquitous in our daily lives, arising from a wide range of materials including clothing, carpets, and furniture [30]. As such, fibre analysis is particularly useful in a forensic context; Zhang et al. have recently used DART-MS for the discrimination of fibre samples [31].

Figure 7 shows the HDM analysis of a polyethylene terephthalate (polyester, PET) fibre. Very few analyte ions were observed until approximately 250 °C, where two distinct ions were noted at 594 *m/z* and 193 *m/z* (Fig. 7i, ii). The ion at 594 *m/z* has been attributed to the ammoniated cyclic trimer of PET [$C_{30}H_{24}O_{12} + NH_4$]⁺, whereas the ion at 193 *m/z* has been assigned to the protonated PET monomer [$C_{10}H_8O_4 + H$]⁺.

Around 250 °C, the fibre was noted to have melted, forming a clear transparent liquid that rapidly darkened to a light brown colour as the fibre began to degrade, seen between micrographs 200 °C and 300 °C. In the same temperature region, the onset of the evolution of analyte ions is noted until around 350 °C as the profiles begin to rapidly decline. Although the analyte ion profiles clearly begin to reduce in their intensity, a sudden spike is noted again shortly after 400 °C. This spike in intensity has been assigned to the formation of a skin on the surface of the polymer (as seen in the micrographs), which reduced the release of gaseous degradation products. Later the skin is seen to burst, and a sudden spike of PET ions is noted before the ion intensities fall away as the fibre is fully degraded. During the second spike of ions, the gaseous build up under the skin of the polymer was likely to include more lower mass degradation products, mainly in the form of the monomer. In contrast, the larger cyclic trimer appears reduced at these elevated temperatures, when compared to the earlier lower temperature melting event when they were more abundant.

Having the ability to visualise the sample as it is heated is a clear benefit, providing explanation to the processes

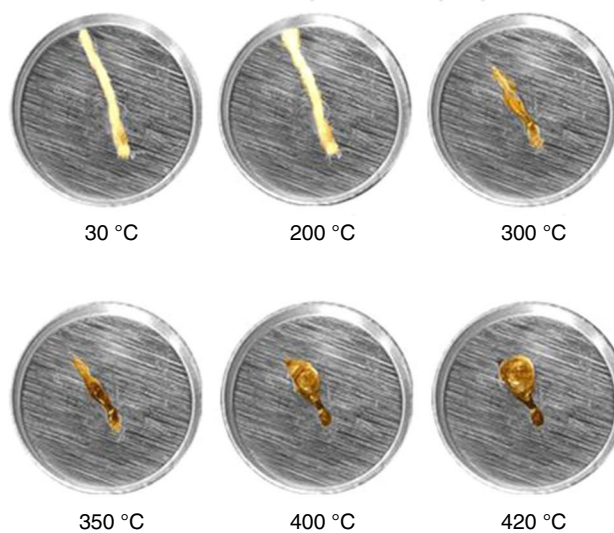
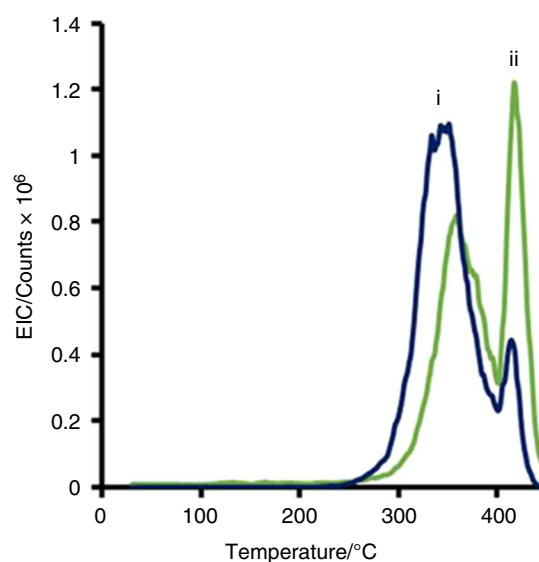


Fig. 7 The analysis of a polyester fibre using HDM. Extracted ion profiles (i) 594 *m/z*, and (ii) 193 *m/z* are plotted as a function of temperature. Selected micrographs and their corresponding temperatures have been shown. (Sample mass, ≈ 1 mg; heating rate, 50 °C min^{-1})

occurring when reviewing complex ion profiles such as those in Fig. 7.

Conclusions

It has been well documented about the clear benefits that can be obtained when analysing a single sample using combined analytical methods. Here, we have demonstrated a complementary analytical technique that combines thermomicroscopy with ambient ionisation mass spectrometry. Examples have been provided that show the clear benefit of being able

to visualise a sample undergoing analysis by mass spectrometry, whilst under controlled heating conditions:

- Trace levels of mixed nitroaromatic compounds were thermally desorbed from brass fibres following surface collection. Here, samples of TNT, PETN and RDX were thermally desorbed, ionised, and separated using a controlled temperature programme.
- The ability to monitor physical processes such as the glass transition and melting point of a 3D printer filament has been demonstrated, showing good correlation with conventional techniques such as DSC and TGA. Additionally, a range of analyte ions linked to polylactic acid oligomers were seen shortly after the melting event was observed.
- Two similarly coloured paint chip samples were analysed using HDM. Although chemically similar, certain unique species could be identified giving a chemical ‘fingerprint’ of each paint chip. The colour information and micrographs gained from the thermal decomposition of the paint chips also showed clear differences aiding in their separation.
- A single polyester fibre was analysed using HDM. During heating, an unexpected spike in the profiles for ions relating to PET was noted. Upon inspection of the micrographs, it was clearly seen that a ‘skin’ had formed on the surface of the liquid polymer, with evident bubbles building under the surface. The temperature at which the skin broke correlated well with the spike observed in the extracted ion profiles.

The combination of thermoanalytical and ambient ionisation methods allows the elucidation of complex thermal processes occurring as a sample is heated. The “soft” ionisation mechanisms associated with techniques such as DART allow for simpler ion identification, when compared to the conventional electron impact mass spectrometry commonly used with thermal analysis.

Author contribution Gage P. Ashton: conceptualisation, methodology, formal analysis, writing – original draft, writing – review and editing; Lindsay P. Harding: conceptualisation, formal analysis, writing – review and editing; Gareth M.B. Parkes: conceptualisation, formal analysis, writing – review and editing.

Open Access This article is licensed under a Creative Commons Attribution 4.0 International License, which permits use, sharing, adaptation, distribution and reproduction in any medium or format, as long as you give appropriate credit to the original author(s) and the source, provide a link to the Creative Commons licence, and indicate if changes were made. The images or other third party material in this article are included in the article's Creative Commons licence, unless indicated

otherwise in a credit line to the material. If material is not included in the article's Creative Commons licence and your intended use is not permitted by statutory regulation or exceeds the permitted use, you will need to obtain permission directly from the copyright holder. To view a copy of this licence, visit <http://creativecommons.org/licenses/by/4.0/>.

References

1. Brown ME. Introduction to thermal analysis. New York: Kluwer Academic Publishers; 2004.
2. Gaisford S, Kett V, Haines P, editors. Principles of thermal analysis and calorimetry. Croydon: Royal Society of Chemistry; 2016.
3. Fernandes RP, et al. Mechanochemical synthesis, characterization, and thermal behavior of meloxicam cocrystals with salicylic acid, fumaric acid, and malic acid. *J Therm Anal Calorim.* 2019;138:765–77.
4. Kanemoto SO, et al. Thermal performance of polyurethane nanocomposite from phosphorus and nitrogen-containing monomer, polyethylene glycol and polydimethylsiloxane for thermal energy storage applications. *J Therm Anal Calorim.* 2021;146:2435–44.
5. Klimesz B, Górecki T, Górecki C. Phase transitions in Ag-based solid electrolytes as detected by thermosonimetry. *Trans Acta.* 2001;374(2):145–9.
6. Charsley EL, Walker C, Warrington SB. Applications of a new quadrupole mass spectrometer system for simultaneous thermal analysis-evolved gas analysis. *J Therm Anal.* 1993;40:983–91.
7. Franguelli FP, et al. Thermal decomposition and spectral characterization of di[carbonatotetraamminecobalt(III)] sulfate trihydrate and the nature of its thermal decomposition products. *J Therm Anal Calorim.* 2021;145:2907–23.
8. Giron D. Applications of thermal analysis and coupled techniques in pharmaceutical industry. *J Therm Anal Calorim.* 2002;68:335–57.
9. Maria TMR, et al. Polymorphism and melt crystallisation of racemic betaxolol, a β -adrenergic antagonist drug. *J Therm Anal Calorim.* 2013;111:2171–8.
10. Ashton GP, Charsley EL, Harding LP, Parkes GMB. Applications of a simultaneous differential scanning calorimetry–thermomicrometry system. *J Therm Anal Calorim.* 2021. <https://doi.org/10.1007/s10973-020-10514-3>.
11. Šimek M, Grünwaldová V, Kratochvíl B. Hot-stage microscopy for determination of API particles in a formulated tablet. *Biomed Res Int.* 2014. <https://doi.org/10.1155/2014/832452>.
12. Bakar MRA, Kalman Nagy Z, Rielly CD. A combined approach of differential scanning calorimetry and hot-stage microscopy with image analysis in the investigation of sulfathiazole polymorphism. *J Therm Anal Calorim.* 2010;99:609–19.
13. Nascimento ALCS, et al. Novel solid-state compounds of heavy rare-earth (III) picolinates. A pyrolytic study using: TG-DSC-IR, HSM-MS and GC-MS. *J Anal Appl Pyro.* 2019;144:104709.
14. Feider CL, Krieger A, DeHoog RJ, Eberlin LS. ambient ionization mass spectrometry: recent developments and applications. *Anal Chem.* 2019;91:4266–90.
15. Takats Z, Wiseman JM, Gologan B, Cooks RG. Mass spectrometry sampling under ambient conditions with desorption electrospray ionization. *Science.* 2004;306:471–3.
16. Cody RB, Laramee JA, Durst HD. Versatile new ion source for the analysis of materials in open air under ambient conditions. *Anal Chem.* 2005;77:2297–302.
17. Venter AR, Douglass KA, Shelley JT, Hasman G Jr, Honarvar E. Mechanisms of real-time, proximal sample processing

- during ambient ionization mass spectrometry. *Anal Chem.* 2014;86:233–49.
18. Wang Y, Sun J, Qiao J, Ouyang J, Na N. A “soft” and “hard” ionization method for comprehensive studies of molecules. *Anal Chem.* 2018;90:14095–9.
 19. Ashton GP, Harding LP, Parkes GMB. An integrated hot-stage microscope–direct analysis in real time–mass spectrometry system for studying the thermal behavior of materials. *Anal Chem.* 2017;89:13466–71.
 20. Charsley EL, Laye PG, Markham HM, Le Goff T. Calibration of differential scanning calorimeters: a comparison between indium and diphenylacetic acid. *Trans Acta.* 2010;497:72–6.
 21. Justes DR, Talaty N, Cotte-Rodriguez I, Cooks RG. Detection of explosives on skin using ambient ionization mass spectrometry. *Chem Commun.* 2007;21:2142–4.
 22. Saha S, et al. Trace level detection of explosives in solution using leidenfrost phenomenon assisted thermal desorption ambient mass spectrometry. *Mass Spectrom.* 2013;2:S0008.
 23. Forbes TP, Verkouteren JR. Forensic analysis and differentiation of black powder and black powder substitute chemical signatures by infrared thermal desorption–DART-MS. *Anal Chem.* 2019;91:1089–97.
 24. Forbes TP, Sisco E, Staymates M. Detection of nonvolatile inorganic oxidizer-based explosives from wipe collections by infrared thermal desorption—direct analysis in real time mass spectrometry. *Anal Chem.* 2018;90:6419–25.
 25. Jayanth N, Jaswanthraj K, Sandeep S, Mallaya NH, Siddharth SR. Effect of heat treatment on mechanical properties of 3D printed PLA. *J Mech Behav Biomed Mater.* 2021;123:104764.
 26. Wang P, Zou B, Ding S, Li L, Huang C. Effects of FDM-3D printing parameters on mechanical properties and microstructure of CF/PEEK and GF/PEEK. *Chin J Aero.* 2021;34(9):236–46.
 27. Ujfalusi Z, Attila Pentek R, Told A, Schiffer M, Nyitrai PM. Detailed thermal characterization of acrylonitrile butadiene styrene and polylactic acid based carbon composites used in additive manufacturing. *Polymers.* 2020;12:2960. <https://doi.org/10.3390/polym12122960>.
 28. Ghelardi E, et al. Py-GC/MS applied to the analysis of synthetic organic pigments: characterization and identification in paint samples. *Anal Bioanal Chem.* 2015;407:1415–31.
 29. Maric M, Marano J, Cody RB, Bridge C. DART-MS: a new analytical technique for forensic paint analysis. *Anal Chem.* 2018;90:6877–84.
 30. Gray FM, Smith MJ, Silva MB. Identification and characterization of textile fibers by thermal analysis. *J Chem Edu.* 2011;88(4):476–9.
 31. Liang J, Frazier J, Benefield V, Chong NS, Zhang M. Forensic fiber analysis by thermal desorption/pyrolysis–direct analysis in real time–mass spectrometry. *Anal Chem.* 2020;92(2):1925–33.

Publisher's Note Springer Nature remains neutral with regard to jurisdictional claims in published maps and institutional affiliations.